Available online at www.sciencedirect.com
ScienceDirect
Lithos 91 (2006) 35–45
LITHOS
www.elsevier.com/locate/lithos

Magnetite compositions and oxygen fugacities of the Khibina magmatic system

Igor D. Ryabchikov [a,*], L.N. Kogarko [b]

[a] Institute for Geology of Ore Deposits, Russian Academy of Sciences, Moscow, Russia
[b] Vernadsky Institute of Geochemistry, Russian Academy of Sciences, Moscow, Russia

Received 11 July 2005; accepted 13 March 2006
Available online 15 May 2006

Abstract

Most titanomagnetite in the Khibina alkaline igneous complex, sampled through 500 m of a vertical cross-section, is represented by Ti-rich varieties. The ulvöspinel component is most commonly around 55 mol%, rarely reaching up to 80 mol%.

We calculated an f_{O_2}–T diagram for magnetite + ilmenite + titanite + clinopyroxene + nepheline + alkali feldspar and magnetite + titanite+ clinopyroxene + nepheline + alkali feldspar phase assemblages at a hedenbergite activity of 0.2. The diagram shows that magnetites with 55 mol% of ulvöspinel crystallized at oxygen fugacities just slightly below the quartz–fayalite–magnetite buffer. More Ti-rich varieties crystallized at higher temperatures and slightly lower ΔQMF values, whereas more Ti-poor magnetites crystallized at or below about 650 °C.

Under the redox conditions estimated for the apatite-bearing intrusion of the Khibina complex (close to the QFM buffer), substantial quantities of methane may only form during cooling below 400 °C in equilibrium with magma. However, even at higher orthomagmatic temperatures and redox conditions corresponding to ΔQMF = 0, the hydrogen content in the early magmatic stage is not negligible. This hydrogen present in the gas phase at magmatic temperatures may migrate to colder parts of a solidifying magma chamber and trigger Fischer-Tropsch-type reactions there. We propose therefore, that methane in peralkaline systems may form in three distinct stages: orthomagmatic and late-magmatic in equilibrium with a melt and — due to Fischer-Tropsch-type reactions — post-magmatic in equilibrium with a local mineral assemblage.

Keywords: Oxygen fugacity; Khibina complex; Fe–Ti oxides; Titanite; Alkaline magmas; Hydrocarbons

1. Introduction

Oxygen fugacity is an important parameter controlling the evolution of magmatic systems. It may determine the crystallizing mineral assemblage and thereby govern the path of fractional crystallization. The most striking example of this effect is strong iron enrichment without increase in silica content during the crystallization of tholeiitic basalts at relatively low oxygen fugacities (Fenner trend) and the fast growth of the silica content due to the early crystallization of magnetite (Bowen trend of calk-alkaline magmatic series) under oxidizing conditions (Osborn, 1959; Presnall, 1966). In peralkaline systems, higher redox conditions may favour the crystallization of acmite-rich clinopyroxene, whereas at lower f_{O_2} alkaline amphiboles may appear.

Oxygen fugacity may also control the partitioning of trace elements between melt and solid phases, particularly for elements with variable valency under the

* Corresponding author.
E-mail address: iryab@igem.ru (I.D. Ryabchikov).

0024-4937/$ - see front matter © 2006 Elsevier B.V. All rights reserved.
doi:10.1016/j.lithos.2006.03.007

conditions of magmatic processes. Such elements include for example Eu, V and Cr. Recently, the behaviour of V in komatiites and other magmatic series was shown to be an efficient indicator of redox conditions (Canil, 1997, 1999, 2002).

Oxygen fugacity also controls the speciation of volatile components and their impact on magma genesis and differentiation. It has been suggested by some investigators that reduced C–H–O volatiles initiated partial melting of mantle rocks after their ascent from greater depths and after their oxidation (e.g. Green et al., 1987). In alkaline magmatic systems, oxygen fugacity determines the presence of hydrocarbons and hydrogen which are commonly found in peralkaline, especially agpaitic rocks (Petersilie, 1958; Petersilie and Sørensen, 1970; Ikorsky and Shugurova, 1974; Kogarko, 1977; Kogarko et al., 1986; Markl et al., 2001; Nivin, 2002; Potter et al., 2004; Nivin et al., 2005; Beeskow et al., this issue; Salvi and Williams-Jones, this issue).

Several approaches have been used to estimate oxygen fugacities in magmatic systems. Some of them are based on equilibrium constants for the reactions between components of solid solutions including both ferrous and ferric iron. Pioneering work by Buddington and Lindsley, 1964 presented experimental data for equilibria of Ti-bearing magnetites with ilmenites, allowing simultaneous estimates of temperature and oxygen fugacity from compositions of coexisting Fe–Ti oxides. Later, this method was extended to spinels and ilmenites of more complex compositions by elaborated thermodynamic models of these phases in a multicomponent system (Sack and Ghiorso, 1991). This method has been successfully applied to fresh volcanic rocks, but is not useful for plutonic mineral assemblages due to the fast re-equilibration of Fe–Ti oxides during slow cooling. For plutonic assemblages, it has been suggested to use equilibria of magnetites and ilmenites with ferromagnesian silicates (Frost et al., 1988; Frost and Lindsley, 1991).

Wones, 1989 discussed the significance of the titanite–magnetite–quartz assemblage. He calculated the equilibrium T and f_{O_2} conditions of titanite-involving reactions for pure phases in the system CaO–FeO–Fe_2O_3–TiO_2–SiO_2 at 1 bar. Later, these reactions were studied experimentally (Xirouchakis and Lindsley, 1998). These experimental data were used to refine thermochemical data for titanite, which permitted the complete T–f_{O_2} diagrams for this system to be constructed (Xirouchakis et al., 2001a). The experimental data were also used to estimate f_{O_2} and T for mineral equilibria in some magmatic rocks (Xirouchakis et al., 2001b). Numerous estimates of oxygen fugacities for mantle peridotites and mantle-derived basaltic magmas were performed on the basis of redox reactions between components of magnetite-bearing spinels, olivines and orthopyroxenes (Ryabchikov et al., 1986; O'Neill and Wall, 1987; Ballhaus et al., 1990; Wood et al., 1990; Ballhaus, 1993).

Many authors have addressed the problem of oxygen fugacities in alkaline rocks. On the basis of stability relations between alkaline pyroxenes, amphiboles and aenigmatite it has been suggested that typical values for the Lovozero peralkaline massif are close to the quartz–fayalite–magnetite buffer (Kogarko, 1977). Data on spinels from OIBs, which include many alkaline basalts, nephelinites and melilitites, show relatively high oxygen fugacities, from the QFM buffer to 2 log units above this level (Ballhaus, 1993). Volcanics from Trindade, including late peralkaline differentiates (Ryabchikov and Kogarko, 1994), also show relatively high oxygen fugacities. Extremely high oxygen fugacities were found for high-Mg effusives and dyke rocks (meimechites and alkali picrites) from the Russian Maimecha–Kotuy province of alkaline rocks and carbonatites (Sobolev et al., 1991; Ryabchikov et al., 2002). Even higher oxygen fugacities were estimated for the Gronnedal–Ika Carbonatite–Syenite Complex, South Greenland (Halama et al., 2005).

Low oxygen fugacities, possibly reaching the field of Fe–Ni alloy stability, were reported for the peralkaline Ilimaussaq massif in South Greenland (Markl et al., 2001; Marks and Markl, 2001). It has also been suggested that f_{O_2} rose during the evolution of the Ilimaussaq magmatic system, during the late stages exceeding the QFM buffer (Markl et al., 2001; Marks and Markl, 2001). Thus, alkaline rocks may form under extremely variable redox conditions.

2. Geological background, petrography and sampling strategy

The Khibina magmatic complex in Russia's Kola Peninsula is one of the largest known alkaline intrusions. It has a concentric, zonal structure with well-developed primary igneous layering. There are eight zones in the complex — distinct rings and conical structures formed by successive phases of intrusion. The oldest rocks tend to occur towards the margins with successively younger intrusions encountered towards the center. Phase 1 comprises nepheline and alkali syenites and nepheline syenite–porphyries. Phase 2 consists of massive khibinites (see Table 1 for explanation of rock names), Phase 3 of trachytoid khibinites, Phase 4 of rischorrites (potassium-rich

Table 1
Glossary of the rock types present in the Khibina massif

Khibinite	Nepheline syenite, intermediate between agpaitic and miaskitic varieties with granular or trachytoid texture
Rischorrite	Nepheline syenite with nepheline grains poikilitically enclosed in microcline
Ijolite	Mesocratic nepheline–pyroxene rock
Melteigite	Melanocratic rock composed mainly of alkali pyroxene and nepheline
Urtite	Nepheline-rich rock
Foyaite	Leucocratic nepheline syenite
Juvite	Leucocratic nepheline syenite rich in K-feldspar
Malignite	Melanocratic nepheline syenite

nepheline syenites). Phase 5 is composed of ijolites, melteigites and urtites and includes a stratified complex of rocks containing the well-known apatite ore deposits. Phase 6 consists of medium-grained nepheline syenites, Phase 7 of foyaites, and Phase 8 of carbonatites. Phase 5 of the Khibina Complex is of special interest because of the rich apatite ore it contains. The Phase 5 intrusion is shaped like a conical sheet which outcrops as a discontinuous ring with a diameter of 26–29 km and a length of ~75 km.

The Phase 5 intrusion has been separated into 3 subphases (Zak et al., 1972): pre-ore (I), ore (II) and post-ore (III). Subphase I consists of ijolites interlayered with subordinate amounts of melteigite, urtite, juvite and malignite. Their total thickness is less than 700 m. Subphase II consists of massive feldspathic urtite, ijolite–urtite and apatite ore with a total thickness of 200 to 700 m. Subphase III is from 10 to 1400 m thick and includes leucocratic and melanocratic ijolites and malignites. The principal phosphate ore deposits are found in Subphase II where the apatite-rich rocks are found in the hanging wall of an ijolite–urtite intrusion. Common accessory minerals in the rocks of this phase are magnetite, titanite and apatite. It has been suggested

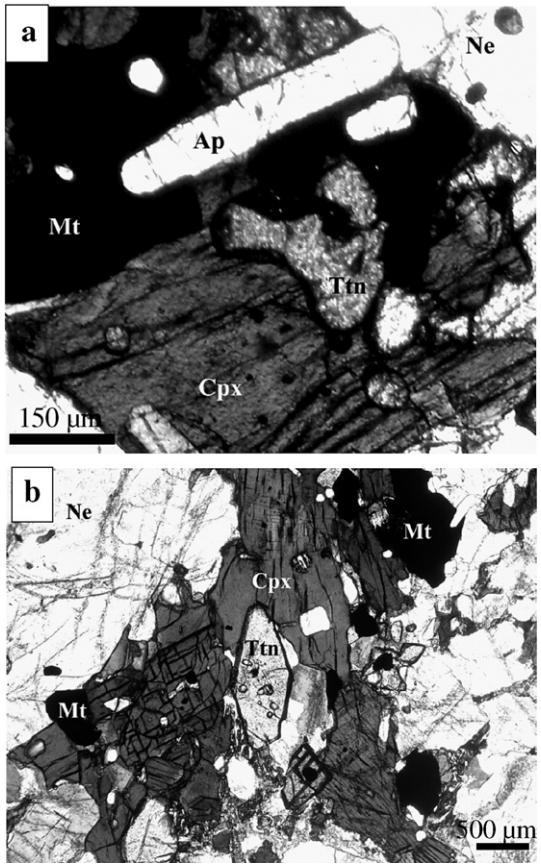

Fig. 1. Clinopyroxene (Cpx), titanite (Ttn), magnetite (Mt) and apatite (Ap) surrounded by nepheline (Ne) in ijolites from the apatite-bearing intrusion of the Khibina complex. a) Aggregate of clinopyroxene, titanite and magnetite with curvilinear equilibrium boundaries. b) Euhedral titanite surrounded by clinopyroxene with magnetite grains near the margins of clinopyroxene.

that apatite crystallized from silicate magma and accumulated in the upper part of the magma chamber due to crystal sorting in the convecting melt (Kogarko,

Table 2
The main rock types in the apatite-bearing intrusion and their modal composition (vol.%)

	Alkali feldspar	Nepheline	Coloured minerals	Ap	Ttn	Mt	Ilm	Coloured minerals
Ijolites	0–15	40–70	20–55	0.5–3	1–5	0.5–5	0–0.5	Cpx
Urtites	0.5–7	75–90	5–25	0.5–10	0.5–10	0.5–1	0–0.5	Arfvedsonite, kataphorite, Lpmln
Melteigites	0–10	10–25	50–60	1–8	1–10	0.5–5	0–0.5	Cpx, arfvedsonite, kataphorite, Lpmln
Malignites	25–35	30–50	15–30	0.5–3	0.5–5	0.5–5	0–0.5	Same
Juvites	20–40	50–65	5–20	0.5–5	0.5–5	0.5–2	0–0.5	Same
Massive apatite ore	0.5–3	1–20	0.5–10	20–95	0.5–5	0.5–1	0.3–0.5	Cpx
Titanite–apatite ore	0.5–3	5–15	5–15	5–30	10–75	3–5	0.5–1	Cpx

Based on publications by Kostyleva-Labuntsova et al. (1978a,b) and Kamenev (1987).
Cpx is clinopyroxene; Lpmln is lepidomelane; Ap is apatite, Mt is magnetite, Ttn is titanite; Ilm is ilmenite.

Table 3
Representative analyses of Fe–Ti oxides, titanites and clinopyroxenes from the ijolite–melteigite–urtite intrusion of the Khibina complex

No.	1	2	3	4	5	6
Mineral	Mt	Mt	Mt	Mt	Mt	Mt
SiO_2	0.42	0.28	0.36	0.33	0.33	0.38
TiO_2	2.85	17.76	19.67	10.34	24.19	18.17
Al_2O_3	0.09	0.10	0.01	0.08	0.05	0.11
Cr_2O_3	0.07	0.05	0.08	0.04	0.05	0.05
FeO	89.71	74.71	72.78	83.02	69.02	75.34
MgO	0.00	0.55	0.01	0.15	0.26	0.28
CaO	0.02	0.00	0.01	0.00	0.00	0.01
Na_2O	na	na	na	na	na	na
K_2O	na	na	na	na	na	na
NiO	0.00	0.00	0.00	0.01	0.00	0.00
MnO	0.29	2.02	2.43	1.17	2.92	2.12
ZnO	0.07	0.13	0.23	0.07	0.20	0.17
V_2O_3	0.40	0.33	0.65	0.26	0.33	0.31
SrO	na	na	na	na	na	na
F	na	na	na	na	na	na
Cl	na	na	na	na	na	na
Total	93.92	95.92	96.23	95.48	97.33	96.94

No.	7	8	9	10	11	12
Mineral	Mt	Mt	Ilm	Ilm	Ttn	Ttn
SiO_2	0.65	0.33	0.24	0.24	30.00	29.74
TiO_2	27.96	13.99	53.26	52.87	37.68	37.54
Al_2O_3	0.03	0.00	0.00	0.00	0.37	0.21
Cr_2O_3	0.04	0.07	0.03	0.05	0.00	0.02
FeO	63.45	78.66	43.18	41.25	1.42	1.14
MgO	0.08	0.08	0.21	0.13	0.00	0.02
CaO	0.01	0.00	0.00	0.02	26.94	26.38
Na_2O	na	na	na	na	0.28	0.40
K_2O	na	na	na	na	na	na
NiO	0.02	0.01	0.01	0.01	na	na
MnO	2.03	1.48	3.99	6.08	0.07	0.07
ZnO	0.05	0.01	0.01	0.10	na	na
V_2O_3	0.21	0.39	0.00	0.00	na	na
SrO	na	na	na	na	0.35	0.59
F	na	na	na	na	0.56	0.64
Cl	na	na	na	na	0.00	0.00
Total	94.53	95.01	100.93	100.73	97.42	96.47

No.	13	14	15	16	17	18
Mineral	Ttn	Ttn	Cpx	Cpx	Cpx	Cpx
SiO_2	29.88	31.57	15	16	17	18
TiO_2	38.76	36.31	52.33	52.09	51.58	51.18
Al_2O_3	0.22	0.79	3.70	2.46	0.78	1.15
Cr_2O_3	0.00	0.00	0.54	0.45	0.44	1.07
Fe_2O_3	na	na	0.01	0.00	0.04	0.00
FeO	0.91	1.28	24.56	25.82	20.75	13.23
MgO	0.00	0.01	0.75	1.09	4.67	9.29
CaO	26.83	25.19	3.33	2.76	13.23	20.24
Na_2O	0.48	1.37	11.78	12.00	6.20	2.58
K_2O	0.08	0.06	0.01	0.00	0.00	0.00
NiO	na	na	0.00	0.00	0.02	0.01
MnO	0.08	0.06	0.78	0.45	0.52	0.57
ZnO	na	na	na	na	na	na

Table 3 (*continued*)

No.	13	14	15	16	17	18
Mineral	Ttn	Ttn	Cpx	Cpx	Cpx	Cpx
V_2O_3	na	na	na	na	na	na
SrO	0.47	0.44	na	na	na	na
F	0.43	0.61	na	na	na	na
Cl	0.00	0.06	na	na	na	na
Total	97.87	97.42	97.78	97.12	98.24	99.32
Mg#	0.00	0.01	0.22	0.40	0.52	0.70

Notes:
(1) Mineral symbols: Mt is magnetite; Ilm is ilmenite, Ttn is titanite, Cpx is clinopyroxene.
(2) FeO is total iron shown as FeO.
(3) Analyses 1 and 10 are for magnetite and ilmenite from an oxyexsolution-like intergrowth.
(4) Analyses 8 and 9 are for larger coexisting ilmenite and magnetite grains.
na means not analyzed.
Mg# is the atomic ratio $Mg/(Mg+Fe^{2+})$.

1977; Kogarko and Khapaev, 1987). The upper parts of the apatite-rich bodies contain titanite–apatite ores (~18% titanite) with elevated Fe–Ti oxide content (>4% magnetite). The main rock types of Phase 5 and their mineral composition are presented in Table 2.

Magnetite and titanite are accessory minerals, present in almost all rock types of the Khibina pluton with the exception of rare lujavrites. Clinopyroxene is the most widespread coloured mineral. Both titanite and clinopyroxene are mainly represented by euhedral grains. Magnetite in many cases also forms euhedral crystals, but may be present as subhedral grains squeezed in between silicate minerals. All three minerals are undoubtedly solid phases crystallized from the magma, and there are no reaction relations among them. They tend to occur in close spatial association in the rocks of the apatite-bearing complex (Kostyleva-Labuntsova et al., 1978b). Aggregates of all three minerals are often composed of grains with curvilinear boundaries (Fig. 1), suggesting that these minerals formed simultaneously during a specific magmatic stage. Magnetite is always more common (up to 11 vol.%) in titanite-rich cumulates in the upper part of this complex. All these observations indicate that magnetite, titanite and clinopyroxene belong to an equilibrium mineral assemblage.

In this study, we analyzed magnetites, titanites and clinopyroxenes from a vertical cross-section of the Phase 5 ijolite–melteigite–urtite intrusion using a core from the Koashva apatite deposit Borehole No. 1312, from the southern part of the Khibina massif. The core covered depths from 450–750 m and intersected rock series underlying the apatite-rich lode. The core contains juvites and feldspathic juvites in the upper part of the

section and ijolites and melteigites in the lower part. Based on data from this core, we calculated the equilibria of magnetite with other minerals to estimate upper and lower limits for oxygen fugacity during their formation.

3. Analytical methods

Minerals from the investigated rocks were analyzed on a JEOL RL-8900 electron microprobe at the Max Planck Institut für Chemie, Abteilung Geochemie, Mainz, Germany, at 20 kV accelerating voltage, 20 nA sample current, and 2 μm beam diameter. Counting times were 30 s for all elements on the peak and 16 s on the background. Natural and synthetic minerals were used as calibration standards. Fe–Ti oxides showing no signs of exsolution under the electron microprobe might have had tiny exsolution features only visible with the TEM. However, nanoscale exsolution features would not have affected our measurements, because the 2 μm electron beam would have integrated their effects.

4. Mineral compositions

Table 3 reports representative analyses of Fe–Ti oxides, titanite and clinopyroxene from the Borehole No. 1312 core. The magnetites show a slight increase in V_2O_5 content towards the lower part of the magmatic body and no other significant compositional trends. The mode of TiO_2 content in the samples is 18–19 wt.%. Similar compositions (17–19 wt.% TiO_2) are typical for magnetites from other parts of the Khibina pluton including apatite ores and titanite–apatite segregations (Kostyleva-Labuntsova et al., 1978b).

Most analyzed magnetite grains are homogeneous. Rarely we found ilmenite intergrowths with a texture similar to oxyexsolution textures. Titanomagnetite and ilmenite occasionally formed larger discrete grains. A number of analyzed grains exhibit higher TiO_2 contents (20–25 wt.%), and one grain has 29 wt.% TiO_2 which corresponds to 85 mol% ulvöspinel. MgO contents in magnetites vary between 0.01 and 0.56 wt.%, and MnO concentrations are relatively high, up to 3 wt.% in Ti-rich varieties. As shown in Fig. 2, the analyzed samples average about 55 mol% ulvöspinel.

Clinopyroxenes in the investigated rocks exhibit a wide range of compositions from diopside-rich (80 mol % of diopside) to acmite-rich varieties (80 mol% of acmite component). The hedenbergite content remains rather constant and is close to 20 mol% (the average of 196 analyses is 19 mol%), and only in late acmite-rich varieties, the hedenbergite content drops significantly. Titanites are characterized by relatively constant composition. In addition to Ca, Ti and Si they contain 0.3–0.8 wt.% Na_2O (average 0.48%), 0.1–0.8% Al_2O_3 (average 0.32%), 1–2% FeO (average 1.25%), 0.1–0.7% SrO (average 0.41%), and 0.4–1% F (average 0.57%). They may also contain 0.5–1% Nb_2O_5+Ta_2O_5, about 0.5% REE, 0.2–0.4% ZrO_2, and possibly some H_2O (Kostyleva-Labuntsova et al., 1978b). We have, however, not analyzed titanites for these elements.

5. Thermodynamic calculations

We estimated f_{O_2} values for the Khibina rocks based on data for the magnetite + ilmenite + titanite + hedenbergite + SiO_2 phase assemblage (Xirouchakis and Lindsley, 1998; Xirouchakis et al., 2001a), corresponding to the reaction

$$3CaTiSiO_5 + 2Fe_3O_4 + 3SiO_2 = 3CaFeSi_2O_6 + 3FeTiO_3 + O_2. \quad (1)$$

These results were obtained for $a_{SiO_2}=1$ and an activity of hedenbergite very close to 1. We recalculated the reaction with lower silica and hedenbergite activities defined by the nepheline + alkali feldspar phase assemblage and compositions of clinopyroxenes present in the Khibina rocks. For this task, we calculated a_{SiO_2} values from the equilibrium constant of the reaction

$$NaAlSiO_4 + 2SiO_2 = NaAlSi_3O_8 \quad (2)$$

Nepheline and albite activities were estimated from the compositions of nepheline and K-feldspar solid solutions present in Khibina melteigites (Kostyleva-

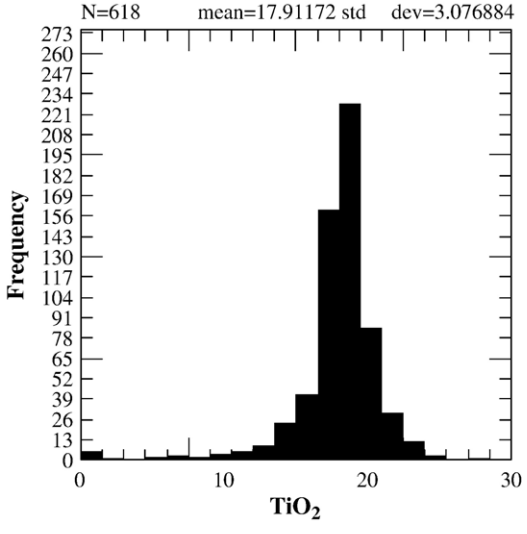

Fig. 2. Histogram of TiO_2 contents in magnetites from Khibina massif, Borehole 1312.

Labuntsova et al., 1978b). Published excess thermodynamic properties of framework silicates were used (Perchuk et al., 1991), Gibbs free energies for substances participating in this reaction are from Shapkin and Sidorov (2003).

Most clinopyroxenes from the apatite-bearing Khibina intrusion have hedenbergite mole fractions around 0.2 (Kostyleva-Labuntsova et al., 1978a,b; Borutsky, 1988; see also Fig. 3). In clinopyroxene solid solutions with substitution of Ca^{2+} by Na^{1+} and Fe^{2+} or Mg^{2+} by Al^{3+}, activity coefficients are ~1 (Perchuk and Aranovich, 1991; Vinograd, 2002). As a first approximation, we therefore assumed that mixing properties of our $CaMgSi_2O_6$–$CaFeSi_2O_6$–$NaFeSi_2O_6$ pyroxenes are close to ideal, and for all our calculations accepted $a_{Hed}=0.2$. We contend that this approximation is a serious source of uncertainty for the estimation of f_{O_2} values. For example, an activity coefficient of 1.5 for hedenbergite in clinopyroxene solid solution would shift oxygen fugacity for phase assemblages with clinopyroxene and titanite towards lower values by half a log unit.

Compositions of titanites in the investigated rocks are relatively constant, and on the average they correspond to the following formula $Ca_{0.948}Na_{0.031}Mn_{0.002}Sr_{0.008}Fe_{0.035}Ti_{0.944}Al_{0.013}Si_{0.996}O_4(O_{0.940}F_{0.060})$. Assuming that the thermodynamics of this phase may be approximated by the ideal multisite mixing model, the estimated activity of $CaTiSiO_4O$ is 0.85. Substitution of this value into the equilibrium constant of reaction (1) shows that oxygen fugacity would be lowered by 0.2 log units by comparison with pure end-member titanite. In fact, due to the ordering of the cation and anion distribution in various structural positions, the activity of the titanite component in the solid solution would be closer to 1.

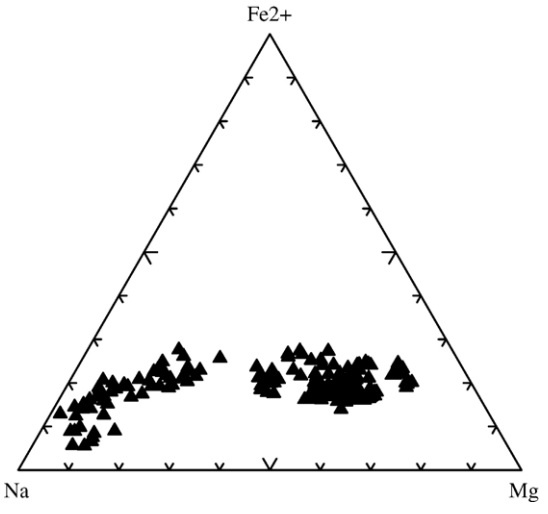

Fig. 3. Triangular diagram for mole fractions of Na, Fe^{2+} and Mg in clinopyroxenes from the rocks in Borehole 1312.

ΔQFM values for various temperatures ($\Delta QFM = \log_{10}(f_{O_2}(\text{rock})/f_{O_2}(QFM)$, where QFM is the quartz–fayalite–magnetite oxygen buffer) were taken from the diagram for 1 bar of Xirouchakis et al. (2001a). Using these values, activities and mole fractions of the Fe_2TiO_4 and Fe_3O_4 components were calculated by the solution of two simultaneous equations based on the equilibrium constants of the reactions:

$$2Fe_3O_4 + 6FeTiO_3 = 6Fe_2TiO_4 + O_2 \quad (3)$$

$$6Fe_2O_3 = 4Fe_3O_4 + O_2 \quad (4)$$

for which a_{usp} and a_{mt} were calculated from the mixing and thermodynamic properties of the end-members of magnetite and ilmenite solid solutions (Ghiorso and Sack, 1991; Sack and Ghiorso, 1991). These values of a_{usp} and a_{mt} together with ΔQFM from Xirouchakis et al. (2001a) were used to calculate for a given temperature the equilibrium constant of the reaction

$$CaFeSi_2O_6 + 3FeTiO_3 = CaTiSiO_5 + 2Fe_2TiO_4 + SiO_2. \quad (5)$$

Subsequently, this equilibrium constant was used to obtain ΔQFM, and the compositions and activities of components in both Fe–Ti oxides at $a_{Hed}<1$ and $a_{SiO_2}<1$. For this, we used the constraint that the value of this equilibrium constant must be the same if $a_{Hed}=1$; $a_{SiO_2}=1$ or $a_{Hed}<1$; $a_{SiO_2}<1$. This permits to find a relation between ilmenite and ulvöspinel activities for these two cases, which may be expressed as $a^2_{usp}/a^3_{ilm}=a^2_{usp(0)}/a^3_{ilm(0)} \cdot (a_{hed}/a_{SiO_2})$, where $a_{usp(0)}$ and $a_{ilm(0)}$ are the previously estimated values of ulvöspinel and ilmenite activities at $a_{Hed}=1$ and $a_{SiO_2}=1$. Using this new value of a^2_{usp}/a^3_{ilm} we solved the simultaneous equations based on the equilibrium constants of reactions (3) and (4) and obtained the compositions of magnetite and ilmenite solid solutions and ΔQFM for a magnetite + ilmenite + titanite + clinopyroxene + nepheline + alkali feldspar phase assemblage at $a_{Hed}<1$ and $a_{SiO_2}<1$.

These values of ΔQFM for the magnetite + ilmenite + titanite + clinopyroxene + nepheline + alkali feldspar phase assemblage are shown by a solid line in Fig. 4. At higher oxygen fugacities, magnetite may be present, but ilmenite is unstable in equilibrium with titanite + clinopyroxene + nepheline + alkali feldspar. At lower oxygen fugacities, there is a magnetite-free field with

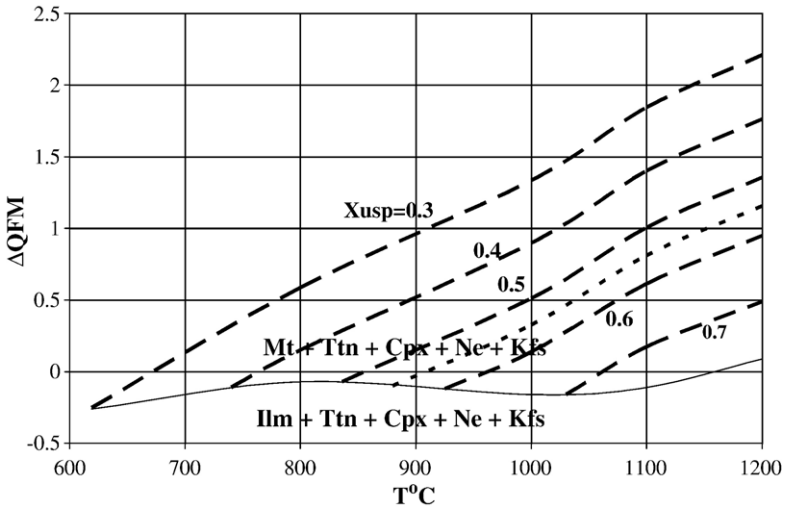

Fig. 4. T - ΔQFM diagram for equilibria of Fe–Ti oxides with titanite, clinopyroxene, nepheline and K-feldspar at $P=1$ bar, activity of hedenbergite equal to 0.2 and a_{SiO_2} buffered by nepheline and K-feldspar with compositions typical of Khibina rocks. The solid line is the univariant reaction for the equilibrium of Ttn+Cpx+Ne+Kfs with both magnetite and ilmenite solid solutions. Dashed lines are isopleths for equilibria among Mt+Ttn+Cpx+Ne+Kfs with fixed X_{usp} values for magnetites.

ilmenite. Thus, when titanite and clinopyroxene are present, the calculated lower limit for magnetite solid solution stability lies at much higher f_{O_2} than when clinopyroxene and titanite are absent. In the absence of titanite and clinopyroxene, the lower limit for magnetite solid solution stability is much lower and is defined by the following reactions:

$$3CaSiO_3 + 3Fe_2TiO_4 + O_2 = 3CaTiSiO_5 + 2Fe_3O_4 \quad (6)$$

$$3Fe_2SiO_4 + O_2 = 2Fe_3O_4 + 3SiO_2. \quad (7)$$

In the ilmenite-free field above Fig. 4's magnetite+ilmenite univariant line, oxygen fugacity is fixed for each temperature and magnetite composition. To find f_{O_2} for various temperatures and magnetite compositions, we recalculated the previously estimated ΔQFM values for the magnetite + ilmenite + titanite + clinopyroxene + nepheline + alkali feldspar phase assemblage to the new composition of magnetite based on the equation for the equilibrium constant of the reaction

$$2CaTiSiO_5 + 2Fe_3O_4 + 2SiO_2 = 2CaFeSi_2O_6 + 2Fe_2TiO_4 + O_2 \quad (8)$$

using the following formula:

$$\Delta QFM = \Delta QFM(i) + 2 \cdot \log_{10}(a_{usp}(i)/a_{mt}(i)/a_{usp} \cdot a_{mt})$$

where ΔQFM(i), a_{usp}(i) and a_{mt}(i) are values for a phase assemblage with ilmenite and magnetite and ΔQFM, a_{usp} and a_{mt} represent an ilmenite-free assemblage for a given magnetite composition. Calculated isopleths of magnetite composition are shown as dashed lines in Fig. 4. As in the case of reaction (5), we have not calculated ΔG of reaction (8) from tabulated thermodynamic data, but only used the fact that the equilibrium constant of this reaction must be the same for a phase assemblage with both ilmenite and magnetite (for which ΔQFM has already been estimated) and for ilmenite-free phase assemblages at the same temperature.

This diagram has been calculated at a pressure of 1 bar, whereas the mineral assemblages in the rocks of the Khibina pluton equilibrated at higher pressures. However, since the oxygen fugacities of Fig. 4 are expressed relative to the QFM buffer, pressure does not affect it significantly because f_{O_2} values for the QFM buffer and for the other redox reactions with ferric and ferrous iron are displaced with increasing pressure in the same direction and approximately to the same extent. Therefore, increase in pressure by 0.1 GPa would shift the calculated ΔQFM values by not more than 0.1 log unit.

Magnetite containing 55 mol% ulvöspinel is the most common composition for the borehole 1312 core sample. For this composition, Fig. 4 shows that magnetite should crystallize at temperatures above 880 °C and oxygen fugacities close to the QFM buffer (ΔQFM= −0.1 at 880 °C and ΔQFM=+0.3 at 1100 °C).

The observed variations in magnetite composition imply that crystallization took place at a range of temperatures and oxygen fugacities. According to Fig. 4, more Ti-rich magnetites with about 25% TiO_2 (70 mol % ulvöspinel, Table 3, analysis 5) would have crystallized above 1030 °C and ΔQFM close to −0.2. The intergrowth of discrete magnetite (40 mol% ulvöspinel) and ilmenite grains (Table 3, analyses 8 and 9) would correspond to 740 °C and ΔQFM= −0.1. Magnetite grains with oxyexsolution textures (Table 3, analyses 1 and 10) crystallized at even lower temperatures.

The most likely temperature range of magnetite crystallization may be assessed from the fact that gravitational sorting in the convecting magma of the Khibina pluton resulted in the accumulation of magnetite together with apatite and titanite in the upper part of the intrusion. This implies that magnetite crystallized simultaneously with apatite. An investigation of melt inclusions in nephelines and apatites from the Khibina intrusion yielded magmatic temperatures of 850–950 °C (Kogarko, 1977) which is consistent with the current estimate of >880 °C for the most common magnetite composition in the borehole No. 1312 core.

Based on our calculations, we estimate oxygen fugacities in this temperature range (850–950 °C) close to the QFM buffer. A similar conclusion was reached for the peralkaline rocks of the Lovozero massif — adjacent to the Khibina massif — based on the relative stabilities of aegirine, arfvedsonite and aenigmatite (Kogarko, 1977). However, a much lower range of oxygen fugacities has been proposed for the Ilímaussaq massif and neighbouring dykes (Markl et al., 2001; Marks and Markl, 2001, 2003). According to these authors, ΔQFM decreased during fractionation in the augite syenite of the Ilímaussaq massif from about −1 to below −4, but increased in the peralkaline stage to values above QFM.

Wide variations of oxygen fugacity in alkaline rocks, with very reducing conditions in local areas, raise the question of whether hydrocarbon-bearing fluids — present in micro-inclusions in minerals of peralkaline rocks — may have formed in the magmatic stage, or whether they could only be produced by non-equilibrium synthesis at low temperatures (Kogarko et al., 1986; Potter et al., 2004; Beeskow et al., this issue; Salvi and Williams-Jones, this issue). We calculated the composition of gas in the C–H–O system at ΔQFM equal to 0 and −3 by simultaneously solving several equations for the equilibrium constants of the following reactions which were calculated from the standard thermodynamic properties of components by Shapkin and Sidorov (2003) and fugacities of gases from Belonoshko and Saxena (1992):

$$CH_4 + O_2 = CO_2 + H_2O \quad (9)$$

$$CO + 0.5O_2 = CO_2 \quad (10)$$

$$H_2 + 0.5O_2 = H_2O. \quad (11)$$

We used the additional constraints $\Sigma X_i = 1$ and $(4X_{CH_4} + 2X_{H_2O} + 2X_{H_2})/(X_{CH_4} + X_{CO_2} + X_{CO}) = 6$. We assumed C/H=6 for all calculations, because many fluid inclusions in alkaline rocks contain substantial amounts of hydrogen in addition to methane (Kogarko et al., 1986; Potter et al., 2004, and our unpublished data).

The results of these calculations are shown in Fig. 5. Even at ΔQFM=0, the hydrogen content at early magmatic temperatures approaches 1 mol%. Methane is low at 900 °C but becomes one of the major species in gas below 400 °C (Kogarko et al., 1986). At ΔQFM= −3, the methane content in the gas is comparable to that of water at both high and low temperatures. The hydrogen content is high at high temperatures (X_{H_2}>0.1 at 900 °C), but falls during cooling. However, even below 400 °C the hydrogen content remains >1 mol% at ΔQFM=−3.

These results indicate that under the very reducing conditions found in some alkaline magmatic systems (Markl et al., 2001), hydrocarbons may be present even at the early magmatic stage through equilibration of the gas phase with the magma. Under more oxidizing conditions — close to QFM buffer as is the case for Khibina magma — methane may form in substantial quantities during cooling below 400 °C in the equilibrium gas phase.

Migration of hydrogen formed at high magmatic temperatures to the cooler parts of the magmatic system facilitated by fast diffusion of H_2 may cause the production of hydrocarbons at lower temperatures by Fischer-Tropsch synthesis. The supply of hydrogen is important for this type of reaction, advocated by some authors for the production of abiogenic hydrocarbons (Kelley, 1996; Potter et al., 2004; Salvi and Williams-Jones, this issue). It has been suggested that hydrogen is produced by dehydration of amphibole in alkaline magmatic systems (Potter et al., 2004). However, this explanation does not seem satisfactory. Hydrogen may appear during amphibole dehydration in substantial quantities only if oxygen fugacity is sufficiently low, which has not been demonstrated for reactions with amphibole in alkaline rocks. There is no convincing

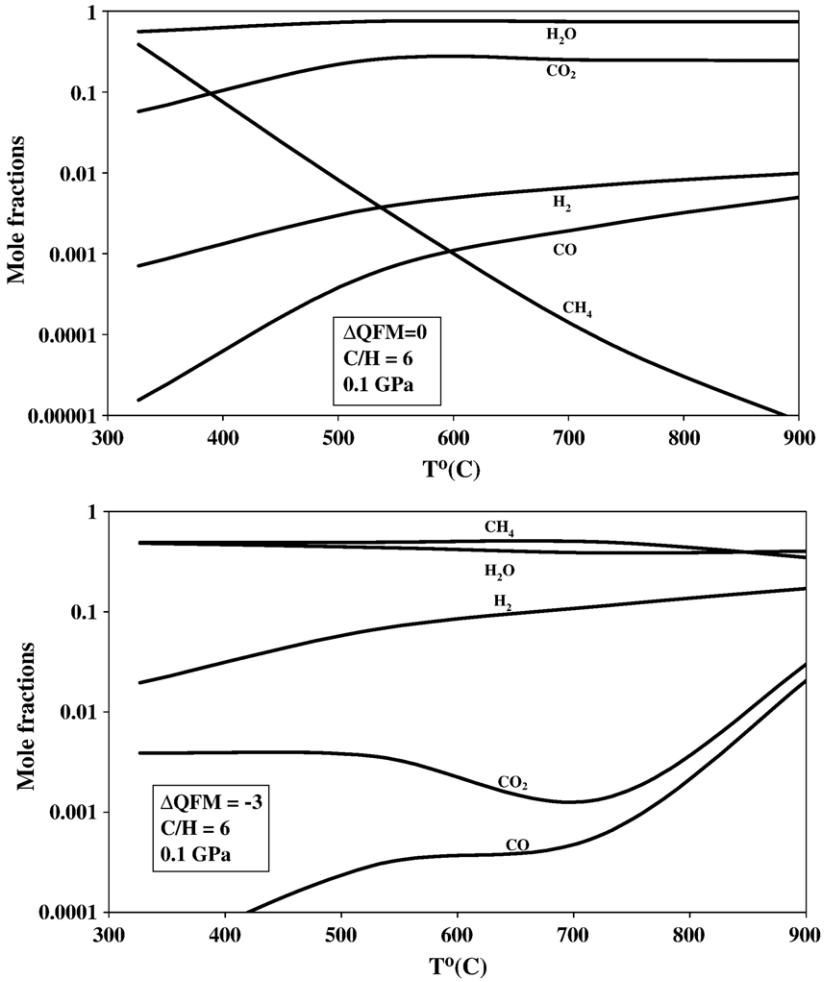

Fig. 5. Composition of the C–H–O gas as a function of temperature at ΔQMF of 0 and −3. P=0.1 GPa. C/H=6.

evidence of widespread amphibole dehydration in Khibina or Lovozero, partly because amphiboles present in these rocks are fluor-amphiboles with low water contents. In our opinion, migration of hydrogen from hot to cold parts of a magmatic system, triggering Fischer-Tropsch synthesis, is a more plausible mechanism.

6. Conclusions

1. Most magnetite in the Khibina alkaline igneous complex, sampled through a vertical cross-section of 500 m, is represented by Ti-rich varieties with typical ulvöspinel contents of about 55 mol%. In rare cases, ulvöspinel reaches 80 mol%.
2. The calculated f_{O_2}–T diagram (Fig. 4) shows that magnetites with 55 mol% of ulvöspinel component in equilibrium assemblages with clinopyroxene and titanite crystallize above 900 °C at oxygen fugacities just below the quartz–fayalite–magnetite buffer. More Ti-rich varieties crystallize at higher temperatures and lower ΔQMF, while more Ti-poor magnetites crystallize at or below 650 °C.
3. Under the redox conditions estimated for the apatite-bearing intrusion of the Khibina complex — close to the QFM buffer — methane may form in substantial quantities during cooling below 400 °C in the equilibrium gas phase. However, even at ΔQMF= 0, the hydrogen content at orthomagmatic temperatures is not negligible.
4. Under very reducing conditions found in some alkaline magmatic systems (Markl et al., 2001), hydrocarbons may be present even at high, orthomagmatic temperatures as a result of equilibration of the gas phase with magma.
5. Hydrogen present in a gas phase at magmatic temperatures may migrate to colder parts of a solidifying

magma chamber and trigger Fischer-Tropsch-type synthesis there.

Acknowledgements

This work has been financially supported by the Russian Foundation for Basic Research, Projects 05-05-64175 and 05-05-64144. The authors are grateful to Gregor. Markl, two anonymous reviewers and Brennan Klose for the constructive criticism, useful suggestions and considerable linguistic improvement.

References

Ballhaus, C., 1993. Redox states of lithospheric and asthenospheric upper mantle. Contributions to Mineralogy and Petrology 114, 341–348.

Ballhaus, C., Berry, R.F., Green, D.H., 1990. Oxygen fugacity controls in the Earth's upper mantle. Nature 348, 437–440.

Beeskow, B., Treloar, P.J., Rankin, A.H., Vennemann, T.W., Spangenberg, J., 2006. A reassessment of models for hydrocarbon generation in the Khibiny nepheline syenite complex, Kola Peninsula, Russia. Lithos 91 (1), 1–18 (this issue).

Belonoshko, A., Saxena, S.K., 1992. Equations of state of fluids at high temperature and pressure (water carbon dioxide, methane, oxygen, and hydrogen). In: Saxena, S.K. (Ed.), Thermodynamic Data: Systematics and Estimation (Adv Phys Geochem, v.10). Springer-Verlag, New York, pp. 79–97.

Borutsky, B.E., 1988. Rock-forming minerals of highly alkaline complexes. Nauka Publishers, Moscow. (in Russian) 215 pp.

Buddington, A.F., Lindsley, D.H., 1964. Iron–titanium oxide minerals and synthetic equivalents. Journal of Petrology 5, 310–357.

Canil, D., 1997. Vanadium partitioning and the oxidation state of Archean komatiite magmas. Nature 389, 842–845.

Canil, D., 1999. Vanadium partitioning between orthopyroxene spinel and silicate melt and the redox states of mantle source regions for primary magmas. Geochimica et Cosmochimica Acta 557–572.

Canil, D., 2002. Vanadium in peridotites, mantle redox and tectonic environments: Archean to present. Earth and Planetary Science Letters 195, 75–90.

Frost, B.R., Lindsley, D.H., 1991. Occurence of iron–titanium oxides in igneous rocks, in: Oxide minerals: petrologic and magnetic significance. In: Lindsley, D.H. (Ed.), Reviews in mineralogy. Mineralogical Society of America, Washington D. C., pp. 433–467.

Frost, B.R., Lindsley, D.H., Andersen, D.J., 1988. Fe–Ti oxide–silicate equilibria: assemblages with fayalitic olivine. American Mineralogist 73, 727–740.

Ghiorso, M.S., Sack, R.O., 1991. Thermochemistry of the oxide minerals. In: Lindsley, D.H. (Ed.), Oxide minerals: petrologic and magnetic significance. Reviews in Mineralogy. Mineralogical Society of America, Washington D.C., pp. 221–264.

Green, D.H., Falloon, T.J., Taylor, W.R., 1987. Mantle-derived magmas — roles of variable source peridotite and variable C–O–H fluid compositions. In: Mysen, B.O. (Ed.), Magmatic processes: physicochemical principles. Geochem. Soc. Spec. Pub., pp. 139–154.

Halama, R., Vennemann, T., Siebel, W., Markl, G., 2005. The Gronnedal–Ika Carbonatite–Syenite Complex, South Greenland: Carbonatite Formation by Liquid Immiscibility. Journal of Petrology 46 (1), 191–217.

Ikorsky, S.V., Shugurova, N.A., 1974. New data on the composition of gases in minerals of the alkaline rocks of the Khibina Massif. Geokhimiya (6), 953–947 (in Russian).

Kamenev, E.A., 1987. Structures of ore fields of the Khibina apatite–nepheline deposits. Prospecting and geological–industrial evaluation of the Khibina type apatite deposits (methodical basis). Nedra, Leningrad, p. 188 (in Russian).

Kelley, D.S., 1996. Methane-rich fluids in the oceanic crust. Journal of Geophysical Research 101 (B2), 2943–2962.

Kogarko, L.N., 1977. Problems of the genesis of agpaitic magmas. Nauka Publishers, Moscow. (in Russian) 294 pp.

Kogarko, L.N., Khapaev, V.V., 1987. The modelling of the formation of apatite deposits of the Khibina massif (Kola Peninsula). In: Parsons, I. (Ed.), Origins of igneous layering. Reidel Publishing Company, Dordrecht, pp. 589–611.

Kogarko, L.N., Kosztolanyi, C., Ryabchikov, I.D., 1986. Geochemistry of the reduced fluid of alkaline magmas. Geokhimiya 1688–1695 (in Russian).

Kostyleva-Labuntsova, E.E., et al., 1978a. Mineralogy of the Khibina massif (magmatism and postmagmatic formations), vol. 1. Nauka Publishers, Moscow. (in Russian) 228 pp.

Kostyleva-Labuntsova, E.E., et al., 1978b. Mineralogy of the Khibina massif (minerals), vol. 2. Nauka Publishers, Moscow. (in Russian) 586 pp.

Markl, G., Marks, M., Schwinn, G., Sommer, H., 2001. Phase equilibrium constraints on intensive crystallization parameters of the Ilimaussaq complex, South Greenland. Journal of Petrology 42, 2231–2258.

Marks, M., Markl, G., 2001. Fractionation and assimilation processes in the alkaline augite syenite unit of the Ilimaussaq intrusion, South Greenland, as deduced from phase equilibria. Journal of Petrology 42, 1947–1969.

Marks, M., Markl, G., 2003. Ilimaussaq 'en miniature': closed system fractionation in an agpaitic dyke rock from the Gardar Province, South Greenland (contribution to the mineralogy of Ilimaussaq no. 117). Mineralogical Magazine 67, 893–920.

Nivin, V.A., 2002. Gas concentrations in minerals with reference to the problem of the genesis of hydrocarbon gases in rocks of the Khibiny and Lovozero massifs. Geochemistry International 40, 883–898.

Nivin, V.A., Treloar, P.J., Konopleva, N.G., Ikorsky, S.V., 2005. A review of the occurrence, form and origin of C-bearing species in the Khibiny alkaline igneous complex, Kola Peninsula, NW Russia. Lithos 85, 93–112.

O'Neill, H.S.C., Wall, V.J., 1987. The olivine-spinel oxygen geobarometer, the nickel precipitation curve and the oxygen fugacity of the upper mantle. Journal of Petrology 28, 1169–1192.

Osborn, E.F., 1959. Role of oxygen pressure in the crystallization and differentiation of basaltic magma. American Journal of Science 257, 609–647.

Perchuk, A.L., Aranovich, L.Y., 1991. Thermodynamics of the jadeite diopside hedenbergite solid-solution model. Geokhimiya (4), 539–547.

Perchuk, L.L., Podlesskii, K.K., Aranovich, L.Y., 1991. Themodynamics of some framework silicates and their equilibria: application to geothermobarometry. In: Perchuk, L.L. (Ed.), Progress in metamorphic and magmatic petrology. Cambridge University Press, Cambridge, pp. 131–164.

Petersilie, I.A., 1958. Hydrocarbon gases and bitumens of the intrusive massifs of the central part of Kola Peninsula. Doklady AN SSSR 122 (6), 1086–1089 (in Russian).

Petersilie, I.A., Sørensen, H., 1970. Hydrocarbon gases and bituminous substances in rocks from the Ilimaussaq alkaline intrusion, South Greenland. Lithos 3, 59–76.

Potter, J., Rankin, A.H., Treloar, P.J., 2004. Abiogenic Fischer-Tropsch synthesis of hydrocarbons in alkaline igneous rocks; fluid inclusion, textural and isotopic evidence from the Lovozero complex, N.W. Russia. Lithos 75, 311–330.

Presnall, D.C., 1966. The join forsterite–diopside–iron oxide and its bearing on the crystallization of basaltic and ultramafic magmas. American Journal of Science 264, 753–809.

Ryabchikov, I.D., Kogarko, L.N., 1994. Redox equilibria in alkaline lavas from Trindade Island, Brasil. International Geology Review 36, 173–183.

Ryabchikov, I.D., Ukhanov, A.V., Ishii, T., 1986. Redox equilibria in upper mantle ultrabasites in the Yakutia kimberlite province. Geochemistry International 23, 38–50.

Ryabchikov, I.D., et al., 2002. Thermodynamic parameters of generation of meymechites and alkaline picrites in the Maimecha–Kotui Province: evidence from melt inclusions. Geochemistry International 40 (11), 1031–1041.

Sack, R.O., Ghiorso, M.S., 1991. An internally consistent model for the thermodynamic properties of Fe–Mg–titanomagnetite–aluminate spinels. Contributions to Mineralogy and Petrology 106, 474–505.

Salvi, S., Williams-Jones, A. 2006. Alteration, HFSE mineralisation, and hydrocarbon formation in peralkaline igneous systems: insights from the Strange Lake Pluton, Canada. Lithos 91(1), 19–34 (this issue).

Shapkin, A.I., Sidorov, Y.I., 2003. Thermodynamic models in cosmochemistry and planetology. Geochemistry International 41 (Suppl. 1), S1–S144.

Sobolev, A.V., Kamenetskaya, V.S., Kononkova, N.N., 1991. New data on petrology of Siberian meimechites. Geochemistry International (8), 1084–1095.

Vinograd, V.L., 2002. Thermodynamics of mixing and ordering in the diopside–jadeite system: I. A CVM model. Mineralogical Magazine 66 (4), 513–536.

Wones, D.R., 1989. Significance of the assemblage titanite + magnetite + quartz in granitic rocks. American Mineralogist 74, 744–749.

Wood, B.J., Bryndzya, L.T., Johnson, K.E., 1990. Mantle oxidation state and its relationship to tectonic environment and fluid speciation. Science 248, 337–345.

Xirouchakis, D., Lindsley, D.H., 1998. Equilibria among titanite, hedenbergite, fayalite, quartz, ilmenite, and magnetite: experiments and internally consistent thermodynamic data for titanite. American Mineralogist 83 (7–8), 712–725.

Xirouchakis, D., Lindsley, D.H., Andersen, D.J., 2001a. Assemblages with titanite ($CaTiOSiO_4$), Ca–Mg–Fe olivine and pyroxenes, Fe–Mg–Ti oxides, and quartz: Part I. Theory. American Mineralogist 86, 247–253.

Xirouchakis, D., Lindsley, D.H., Frost, B.R., 2001b. Assemblages with titanite ($CaTiOSiO_4$), Ca–Mg–Fe olivine and pyroxenes, Fe–Mg–Ti oxides, and quartz: Part II. Application. American Mineralogist 86, 254–264.

Zak, S.L., et al., 1972. The Khibina alkaline massif. Nedra, Leningrad. (in Russian) 175 pp.